

## Photografting and the Control of Surface Chemistry in Three-Dimensional Porous Polymer Monoliths

Thomas Rohr,<sup>†</sup> Emily F. Hilder,<sup>†</sup> John J. Donovan,<sup>‡</sup> Frantisek Svec,<sup>†,§</sup> and Jean M. J. Fréchet<sup>\*,†,§</sup>

Materials Sciences Division, E.O. Lawrence Berkeley National Laboratory, Berkeley, California 94720; Department of Geological Sciences, University of Oregon, Eugene, Oregon 97403; and Department of Chemistry, University of California, Berkeley, California 94720-1460

Received August 19, 2002

**ABSTRACT:** The photografting of porous three-dimensional materials has been achieved using a benzophenone-initiated surface photopolymerization within the pores of a macroporous polymer monolith contained in a fused silica capillary. Despite the relatively high thickness (100  $\mu\text{m}$  or more) of the layer of material involved, the photografting process occurs efficiently throughout its cross section as confirmed by electron probe microanalysis. In addition, the use of photomasks during grafting enables the precise placement of specific functionalities in selected and predetermined areas of a single monolith for use in a variety of applications ranging from supported catalysis to microfluidics. For example, we have demonstrated the fast and selective incorporation of chains of poly(2-acrylamido-2-methyl-1-propane-sulfonic acid) into the irradiated areas of pores of a 100  $\mu\text{m}$  thick monolith and monitored the extent of grafting through measurements of the electroosmotic flow afforded by the newly introduced ionized functionalities. Grafting of the porous polymer with 4,4-dimethyl-2-vinylazlactone was also successful and could be monitored visually by fluorescence measurements following fluorescent labeling of the grafted chains with Rhodamine 6G.

### Introduction

The grafting of solid surfaces with layers of polymers has become a very important technique used in areas as varied as microelectronic packaging, biochips, or pH-sensitive membranes.<sup>1,2</sup> In these and numerous other applications, surface grafting enables the introduction of specific properties derived from the grafted layer while also preserving the bulk and structural properties of the underlying material. Most previously reported work has involved grafting on readily accessed planar surfaces<sup>1</sup> but not through thick layers or deep within the pores of bulk material encased in a sheathing substrate.

Given the growing interest in microfabricated devices designed for micrototal analytical systems ( $\mu\text{-TAS}$ )<sup>3,4</sup> and the inherent limitations of microfluidic chips with open channel architecture, a configuration with very low surface-to-volume ratio, the grafting of active polymer surfaces on the walls of such chips could considerably increase their functional capabilities. In particular, applications such as chromatographic separations, heterogeneous catalysis, and solid phase extraction that rely on interactions with a solid surface would greatly benefit from the introduction of multiple functionalities emanating from the walls of the channels and permeating throughout their inner volume. An appealing approach would involve the packing of channels with functionalized porous particles as this would significantly increase the available surface area and enable the introduction of specific chemistries into the device. While this approach would indeed solve the issue of limited surface area in the devices, it is best suited for

macroscopic devices such as HPLC columns, but it is difficult to implement for the mass production of microfluidic systems. As a result, only a few reports have dealt with attempts to enhance the limited surface area in channels of a microchip by packing them with small beads or by fabricating arrays of ordered features within their channels.<sup>5–9</sup>

In the early 1990s, we have developed a novel and extremely versatile format of porous materials: rigid macroporous polymer monoliths.<sup>10,11</sup> These materials with well-controlled porous properties are prepared by in-situ polymerization within the confines of a cavity, for example, a chromatographic column, acting as a mold. Monoliths have now been used in a broad range of applications that frequently take advantage of the fact their large pores allow liquid flow at low applied pressures.<sup>11–13</sup> However, monoliths with very large pores typically have limited surface areas and therefore only present a limited amount of functional groups at their surfaces. We have therefore attempted to implement the controlled and radially uniform grafting of chains of functional polymers within the large pores of cylindrical polymer monoliths as this would provide a versatile access to permeable materials with both tailored surface chemistries and controlled extent of functional group incorporation.<sup>14</sup> The grafted materials would then possess the high loading of functional groups that would make them attractive for a variety of applications involving flow through a reactive solid polymer (e.g., catalysis, capture, molecular recognition, and separation). In early work we have used active initiating or polymerizable sites located on the surface of the porous matrix to effect grafting.<sup>15</sup> Therefore, the primary coverage of the pore surface with these active sites had a decisive effect on the efficiency of the grafting. Changing the concentration of such active sites in the original monoliths is not an easy process as any

<sup>†</sup> E.O. Lawrence Berkeley National Laboratory.

<sup>‡</sup> University of Oregon.

<sup>§</sup> University of California.

\* Corresponding author: Tel 510 643 3077; fax 510 643 3079; e-mail [frechet@cchem.berkeley.edu](mailto:frechet@cchem.berkeley.edu).

change in composition during the preparation of the monoliths translates into significant changes in their porous structure. In addition, the use of heat to initiate grafting usually leads to functionalization of the entire monolith and therefore does not enable the precise placement of grafted sections in predetermined and highly localized areas of the porous matrix.

In this report we demonstrate that despite the irregular and highly scattering nature of the porous monoliths, photografting can be used for their fast, efficient, and versatile surface functionalization. In addition, we show that the use of simple photomasks precisely positioned atop of the monolith enables the grafting to proceed strictly in those confined areas of the monolith that are exposed to radiation while no functionalization is observed in dark areas. This process permits the introduction of multiple sites with various functionalities located next to each other or at predetermined locations in a single monolith. This three-dimensional patterning process, which is analogous to the standard photolithography used in microelectronics, may also be used to create axial gradients or layers of functionalities not accessible by using any other technique. The use of this photografting approach is expected to significantly enhance access to highly functionalized reactive surfaces in applications such as microfluidics, chromatography, or catalysis.

## Results and Discussion

**Control of Porous Properties.** Porous properties are important for all applications of molded polymer monoliths, since they are generally designed to operate in a flow-through mode. Therefore, our initial studies of monolithic materials focused on the fine control of their porosity. However, the thermally initiated free radical polymerization we used in much of our earlier work is not ideally suited for the preparation of segments of monolithic structures within microdevices since the selective heating of specific areas of the microchip to position the monolith strictly within the assigned space is difficult to achieve. This issue was subsequently addressed by the development of UV-initiated polymerization processes similar to the photolithographic patterning used in microelectronics.<sup>16–19</sup> Photopolymerization enables the formation of monoliths only within one or more specified spaces. The polymerization reaction is strictly confined to those areas exposed through the clear, light-transmitting portion of a mask, while no polymerization occurs in the dark areas of the mask.

A number of variables are available to control the porous properties of macroporous materials prepared using photopolymerization, including the irradiation time, lamp power, percentage of cross-linker, concentration of initiator, and composition and percentage of the porogenic solvent.<sup>20</sup> In this study, we used a binary porogenic solvent consisting of 1-decanol and cyclohexanol or 1,4-butanediol that enables the fine control of the porous structure in systems containing butyl methacrylate and ethylene dimethacrylate. In all cases the polymerization mixture contained 16% of cross-linker, 24% of monovinyl monomer, and 60% porogens, and the photopolymerizations were carried out at room temperature (Table 1). To further simplify the design of our experiments, 1 wt % (with respect to monomers) of the free radical photoinitiator (2,2-dimethoxy-2-phenylac-

**Table 1. Compositions of Polymerization Mixtures Used for the Preparation of Porous Polymer Monoliths**

	monoliths series	
	I	II
butyl methacrylate, wt %	24	24
ethylene dimethacrylate, wt %	16	16
1-decanol, wt %	$x^b$	$x^b$
1-cyclohexanol, wt %	$60 - x$	
1,4-butanediol, wt %		$60 - x$
DMAP, wt % <sup>a</sup>	1	1

<sup>a</sup> Percentage of 2,2-dimethoxy-2-phenylacetophenone with respect to monomers. <sup>b</sup> Percentage of 1-decanol was varied in the range of 20–60 wt %.

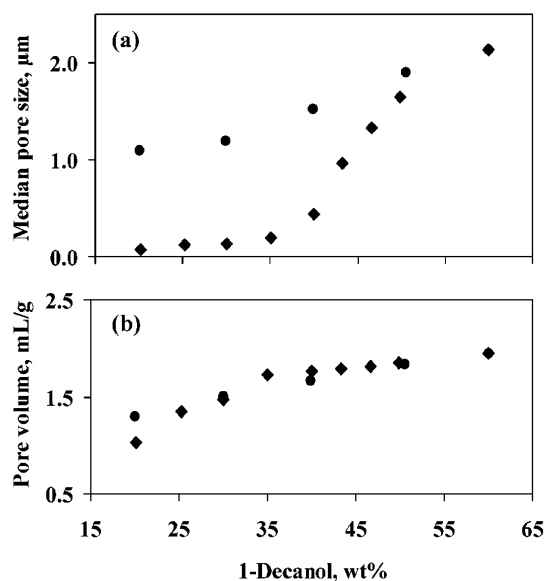


**Figure 1.** Effect of percentage of decanol on median pore size (a) and pore volume (b) in polymerization mixtures containing cyclohexanol (◆) and 1,4-butanediol as co-porogens (●). Polymerization mixture: butyl methacrylate, 24%; ethylene dimethacrylate, 16%; porogens, 60%; 2,2-dimethoxy-2-phenylacetophenone, 1% (with respect to monomers); irradiation time, 10 min; temperature, 20 °C.

etophenone) was used throughout. Thus, the composition of porogenic solvent was the only variable used to control porous properties in our experiments. Figure 1 shows the effect of the percentage of decanol in the porogenic solvent mixture with either co-porogen (cyclohexanol or butanediol) on both the median pore size and the pore volume of the resulting monoliths. Clearly, these experiments demonstrate the broad dynamic range of pore sizes that can easily be achieved by simple adjustments in the composition of porogenic solvent. The S-shaped plot of pore sizes starts at very small values of about 70 nm for a 20:40 mixture of decanol and cyclohexanol and reaches its maximum at 2100 nm for mixtures containing only decanol with no co-porogen. Replacing of cyclohexanol with butanediol enables the preparation of monoliths with larger pores even at low percentages of decanol. For example, a large pore size of 1000 nm is obtained using a polymerization mixture containing only 20% decanol and 40% butanediol while more than 45% decanol would have to be used in combination with cyclohexanol to achieve this pore size. In contrast to its effect on pore size, the type of porogen used has only a small effect on the pore volume since, at the end of the polymerization, the fraction of pores within the final porous polymer is close to the volume fraction of the porogenic solvent in the initial polymer-

**Table 2. Reaction Mixtures Used for Photografting of Monoliths with 2-Acrylamido-2-methyl-1-propanesulfonic Acid (AMPS) and 4,4-Dimethyl-2-vinylazlactone (VAL)<sup>a</sup>**

mixture	solvent	monomer, wt %		initiator, wt % <sup>b</sup>	Pluronic F-68, wt %
		AMPS	VAL		
A	H <sub>2</sub> O	15		0.02	0.34
B	tBuOH–H <sub>2</sub> O 3:1	15		0.22	
C	tBuOH		15	0.22	

<sup>a</sup> For other conditions see Experimental Section. <sup>b</sup> Concentration of benzophenone in solution.

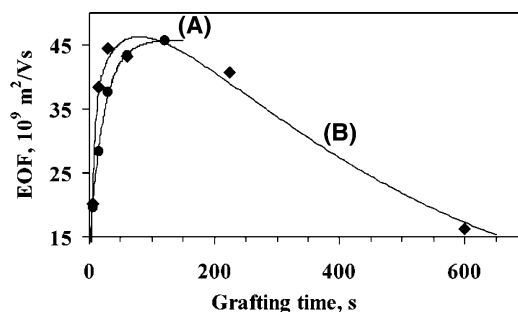
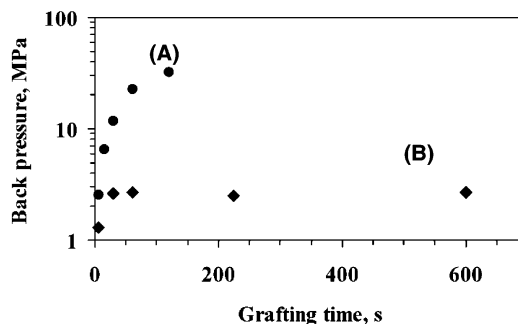
ization mixture because the porogen remains trapped in the voids of the monolith during its formation.

**Surface Grafting of 2-Acrylamido-2-methyl-1-propanesulfonic Acid.** The mechanism of photografting onto polymer films using aromatic ketones such as benzophenone as photoactive component has been elucidated by Rånby.<sup>21</sup> According to Rånby's mechanism, excitation of the photoinitiator by UV light at 200–300 nm ultimately leads to hydrogen abstraction and formation of a free radical on the polymer substrate. This energy-rich radical then initiates propagation reaction, leading to grafting from the surface. The counterpart semipinacol radical formed simultaneously from the initiator does not have sufficient energy to initiate polymerization in solution to any significant extent and is mostly quenched by combination, leading to its dimerization or termination of the growing polymer chains. Since the growing polymer chains grafted to the surface also contain abstractible hydrogen atoms, these new chains also serve as loci from which new chains can grow, ultimately leading to a branched polymer architecture.

We have previously demonstrated that surface photografting using a wide variety of different monomers initiated by free radicals generated from aromatic ketones is suitable for the functionalization of channels within microfluidic devices fabricated from thermoplastics.<sup>22</sup> The reaction conditions for this grafting were optimized to obtain surfaces modified with various functionalities quickly and efficiently. These optimized conditions could be easily adjusted to achieve efficient grafting of pore surface in the porous polymer monoliths.

Since this project is closely related to our ongoing studies in electrochromatography, we choose 2-acrylamido-2-methyl-1-propanesulfonic acid (AMPS) as the model monomer for photografting. Its ionizable character also enables the use of electroosmotic flow (EOF), which is largely independent of the pore size, to monitor the extent of grafting. Monoliths with a pore size of 1.5  $\mu\text{m}$  prepared within 100  $\mu\text{m}$  i.d. fused silica capillaries from a polymerization mixture containing butanediol were selected for grafting with AMPS. Since the benzophenone photoinitiator has very low water solubility, we added a surfactant (Pluronic F-68) to enable the use of higher concentrations of initiator after homogenization. Since emulsions containing more than 0.02% of initiator tended to be turbid, affecting the reproducibility of results, we only used clear solutions with 0.02% initiator for the grafting of porous monoliths with AMPS. Such experiments (Table 2, mixture A) afforded very reproducible results.

Figures 2 and 3 show the effect of grafting time on the electroosmotic flow and the back pressure in the capillaries, respectively. As expected, using conditions A (Table 2), EOF initially increases with increasing

**Figure 2.** Effect of grafting time on electroosmotic flow (EOF) for monoliths grafted with 2-acrylamido-2-methyl-1-propanesulfonic acid in water (mixture A, Table 2) (●) and in *tert*-butyl alcohol/water (mixture B, Table 2) (◆).**Figure 3.** Effect of grafting time on back pressure measured with water at a flow rate of 0.1  $\mu\text{L}/\text{min}$  for monoliths grafted with 2-acrylamido-2-methyl-1-propanesulfonic acid in water (mixture A, Table 2) (●) and in *tert*-butyl alcohol/water (mixture B, Table 2) (◆).

irradiation time and appears to level out after about 1 min. The initial rapid increase in EOF indicates that the extent of surface modification of the porous matrix is controlled by the grafting time. The increasing number of ionized functionalities grafted to the surface leads to an increase in electroosmotic flow. Once the grafted polymer layer reaches a certain thickness, only those functionalities that are located at or near the surface of that layer contribute to the electroosmotic flow. Since their number becomes effectively independent of the thickness of the underlying layer, EOF does not change any longer. The continuous increase in flow resistance with the grafting time, measured as the back pressure of water pumped through the monolith, shown in Figure 3 is a good indication that the thickness of the grafted layer increases. A very high back pressure of 33 MPa was observed for a monolith 8.5 cm in length after a grafting time of 2 min. This extent of grafting made pumping solvents through the monolith and washing the pores very difficult. As a result, no attempt was made to use longer grafting times. However, despite these extremely high pressures, we did not observe any physical damage or dislocation of the monolith, confirming its high mechanical stability and its firm attachment to the walls of the housing.

The electron micrograph of the morphology of a monolith grafted with AMPS for 1 min—the reaction time that affords permeable monoliths while still enabling washing at a tolerable back pressure—does not reveal any significant differences compared to the parent monolith (Figure 4). This suggests that the polyAMPS layer is rather thin in the dry state (used to obtain the micrograph) and that the high resistance to pressurized flow (pumping) is likely the result of the swelling of the highly branched hydrophilic polyAMPS

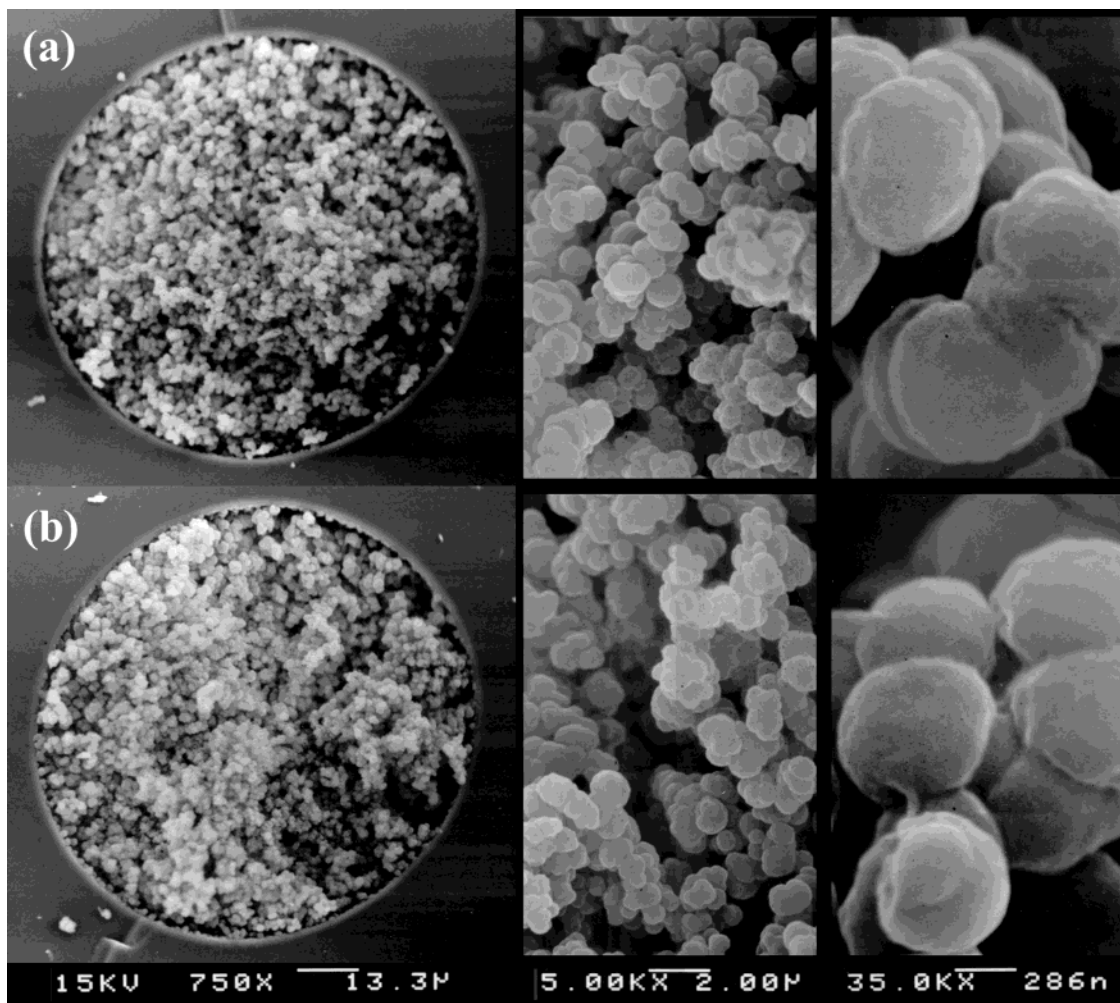


**Figure 4.** SEM images of the generic monolith with a pore size of  $1.5 \mu\text{m}$  before (a) and after 1 min grafting with 2-acrylamido-2-methyl-1-propanesulfonic acid in water (b).

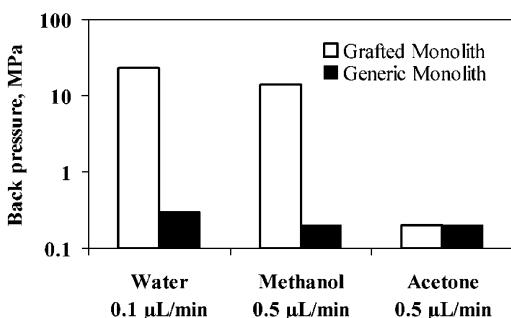


**Figure 5.** Back pressure exerted in various solvents by generic monolith with a pore size of  $1.5 \mu\text{m}$  and a length of 8.5 cm and the same monolith grafted with 2-acrylamido-2-methyl-1-propanesulfonic acid using reaction conditions A (Table 2) and a grafting time of 1 min.

grafts in water. This conclusion is supported by back pressure measurements using different solvents. As shown in Figure 5, a back pressure of 23 MPa is observed at a low flow rate of  $0.1 \mu\text{L}/\text{min}$  when water is pumped through the monolith grafted for 60 s, while the back pressure is only 14 and 0.2 MPa when methanol or acetone is used, respectively, at the higher flow rate of  $0.5 \mu\text{L}/\text{min}$ . Obviously, these solvents do not swell polyAMPS grafts to the same extent as water, and therefore the pores are less clogged, leading to a lower back pressure. These values also correlate well with the solubility parameters of these solvent which are 47.9,

29.7, and  $20.1 \text{MPa}^{1/2}$  for water, methanol, and acetone, respectively.<sup>23</sup> For comparison, the flow resistance of the original ungrafted monolith under equal conditions is in the range 0.2–0.3 MPa for all three solvents.

Irwan et al.<sup>24</sup> have recently observed that the extent of swelling of poly(methacrylic acid) photografted onto a polyethylene film depends strongly on the solvent used for grafting. Therefore, we tested this approach to see whether the period of time used for grafting might be extended without clogging the pores. However, our choice of suitable solvents is limited by the specifics of the photoinitiated grafting. The desirable solvent (i) should have a low absorbance in the UV range to exert minimum self-screening effect, (ii) should not be subject to hydrogen abstraction, since this would both lead to its incorporation into the polymer layer by termination reactions and interfere with the desired graft polymerization, and (iii) must dissolve all components of the polymerization mixture (monomer and initiator). *tert*-Butyl alcohol (tBuOH) and its mixtures with water meet all these criteria, since *tert*-butyl alcohol is a good solvent for numerous monomers as well as for benzophenone (initiator).

Figure 6 illustrates the proposed grafting process. Initially, only a limited number of polymer chains grow from the surface (a). As the polymerization continues, the degree of branching increases since grafting also occurs via H-abstraction from the already grafted chains (b). As the density of chains increases, cross-linking

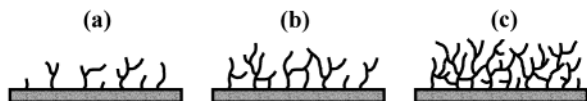


**Figure 6.** Schematic representation of the growing polymer chains during photografting with increasing irradiation time from (a) to (c).

becomes increasingly prevalent, and finally, a dense cross-linked polymer network is formed (c). Considering the nature of the grafting reactions forming a polymer layer cross-linked via intermolecular termination reactions of the branched polymer chains, the cross-linking density must clearly depend on the distance between the individual chains. Thus, the least cross-linked layer may be expected to form from chains that are highly solvated with water. In contrast, solvation is much less extensive when less polar solvents such as tBuOH are used, and as a result, the grafted chains are closer to each other, making the intermolecular cross-linking reactions more likely. Indeed, Figures 2 and 3 demonstrate that a more cross-linked, and therefore less swellable, polyAMPS layer can be grafted using a 75% solution of tBuOH in water (Table 2, mixture B). Using this solvent mixture, the flow resistance remains acceptable even after much longer grafting times and with a higher concentration of initiator. The maximum value of back pressure obtained with this solvent system is reached after about 1 min of grafting and does not change much thereafter, most likely as a result of extensive cross-linking. For example, the monolith grafted for 10 min under these conditions still only exhibits an acceptable back pressure of 2.8 MPa.

EOF also increases during grafting to again reach its maximum value after about 1 min. In contrast to the grafting reaction performed from water/Pluronic solution, the grafting time could easily be extended to 10 min, thus enabling monitoring of its effect on EOF over a much broader range. Surprisingly, the electroosmotic flow shown in Figure 2 quickly reaches a maximum value of  $45 \times 10^{-9} \text{ m}^2/(\text{V s})$  and then decreases to about one-third of this value after 10 min of grafting time.

#### Homogeneity of Grafting in Polymer Monoliths.

Our previous work has shown that the photografting of surfaces could easily be achieved with bulk monomers

even when irradiation is done through a  $200 \mu\text{m}$  thick layer of monomer.<sup>22</sup> However, absorption of UV light by monomers, initiator, solvent, and the polymer matrix itself can affect light intensity, and therefore the extent of grafting polymer may vary within the thickness of the monolith. The use of less absorbing dilute solutions of monomers in solvents such as tBuOH/water can help reduce the self-screening, but radial gradients of functionalities within the grafted monoliths may still be formed.

To quantify any such self-screening effect and the resulting gradient formation, we grafted two capillaries using identical conditions as shown in Table 2 (mixture B, 1 min irradiation) but changing the method of irradiation. While one capillary was revolving at 50 rpm during the grafting procedure, the second was kept stationary while irradiated through a quartz window. The cross sections of these capillaries were then subjected to microprobe analysis for sulfur (Figure 7).

Two perpendicular scans were performed across the cross section of both monoliths, with 50 data points for each measurement. The signal response presented in Figure 7 appears rough because both the pore size and the step length with which the electron beam is moved across the monolith have similar dimensions ( $1\text{--}1.5 \mu\text{m}$ ). Obviously, maxima on the intensity profiles are obtained when the beam hits the polymer microglobules, while almost no signal is monitored when the electron beam is positioned above the pore. Although some minor differences between the two materials can be observed, the sulfur content profiles for the grafted monoliths prepared using the two different irradiation methods are very similar. This indicates that no appreciable gradients are formed during the stationary irradiation of the  $100 \mu\text{m}$  thick monolith. Electrochromatographic separations carried out with these test monoliths also did not reveal any differences between the monoliths grafted using the two different procedures. Since most of the current microfluidic channels have a typical depth of only  $20\text{--}30 \mu\text{m}$  vs the  $100 \mu\text{m}$  used in our control experiments, this finding indicates that the danger of producing nonhomogeneous devices using our grafting procedure is essentially nil.

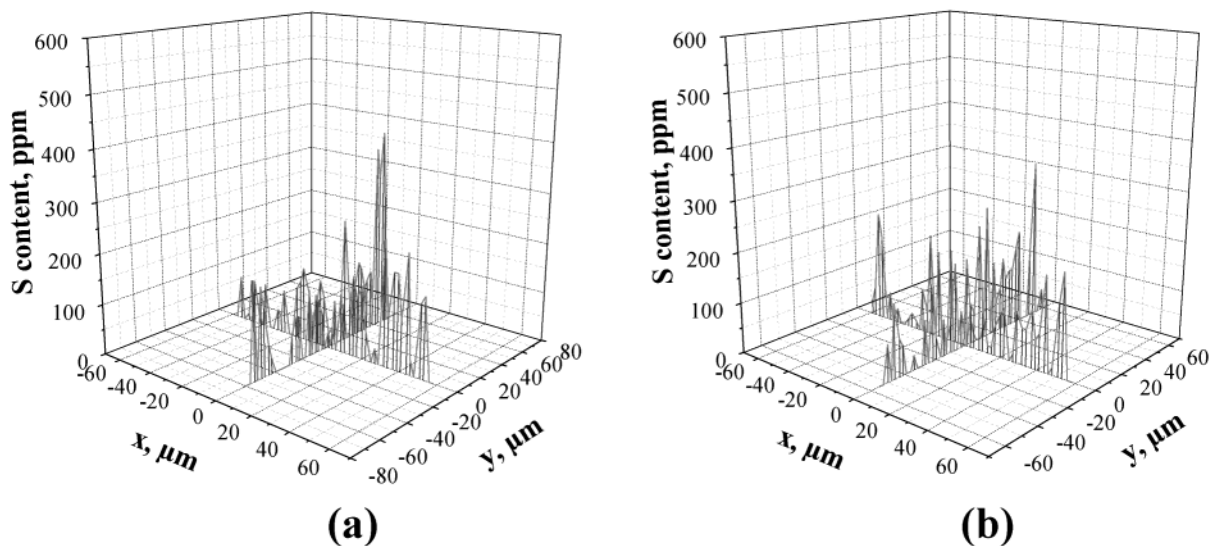


**Figure 7.** Sulfur content of grafted poly(2-acrylamido-2-methyl-1-propanesulfonic acid) determined using electron probe microanalysis. Grafting was performed in stationary (a) and revolving capillary (b).

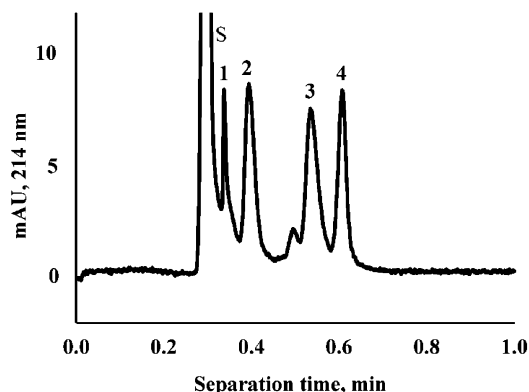


**Figure 8.** Separation of peptides using monolithic capillary grafted with 2-acrylamido-2-methyl-1-propanesulfonic acid. Conditions: capillary column total length 34.5 cm, monolith 8.5 cm, 30 s grafting; mobile phase 100 mmol/L NaCl solution in 10 mmol/L phosphate buffer pH 6.0; voltage  $-15$  kV; overpressure in both vials 0.8 MPa; temperature  $60$  °C; concentration of peptides 0.1 mg/mL; pressure driven injection at 0.8 MPa for 0.05 min. Peaks: system peak (S), Gly-Tyr (1), Val-Tyr-Val (2), methionine enkephalin (3), leucine enkephalin (4).

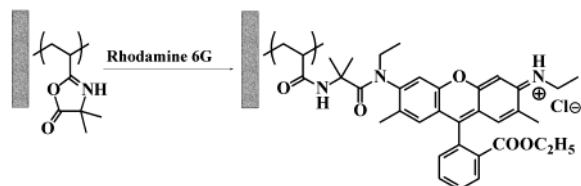


**Figure 9.** Scheme of reaction of Rhodamine 6G with porous polymer monolith containing grafted poly(4,4-dimethyl-2-vinylazlactone) chains.

**CEC Separation of Peptides.** Figure 8 shows as an example separation of peptides in capillary electrochromatographic mode using a monolithic column grafted with AMPS. This isocratic separation is unusually fast, and all four peptides are well separated in less than 1 min. This rapid separation that was achieved with the grafted monolithic stationary phase clearly demonstrates the high magnitude of the electroosmotic flow driven by grafted AMPS chains that is about 2 times as high as that observed for silica-based packings developed specifically for CEC.<sup>25</sup> This can again be attributed to the large number of accessible ionized functionalities located on the surface of the pores.

**Patterning Chemistries in Porous Matrices.** The additional benefit of photografting is the ability to create patterns differing in properties such as surface coverage or even type of grafted chemistry. This is demonstrated by grafting vinylazlactone (VAL) through a mask on a monolith several cm long with  $1.5$   $\mu\text{m}$  pores prepared within a  $50$   $\mu\text{m}$  i.d. capillary. The mask created on a Borofloat glass wafer leaves open windows 1 mm long separated by covered areas also 1 mm long. The reactive functionalities of the grafted chains were then labeled with Rhodamine 6G by reaction with its secondary amino groups as shown schematically in Figure 9. Immobilization of the fluorescent dye enables the visualization of the grafts by optical fluorescence microscope. Figure 10 shows images of the monolith grafted with VAL for 1 and 3 min. The fluorescent areas (bright fields) observed after 1 min irradiation are slightly less than 1 mm long, most likely as a result of light scattering at the edges of the mask features. In contrast, the length of the fluorescent areas after 3 min of

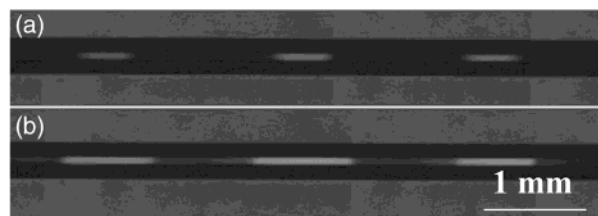


**Figure 10.** Fluorescence microscope image of porous poly(butyl methacrylate-*co*-ethylene dimethacrylate) monolith in a  $50$   $\mu\text{m}$  capillary photografted through a mask with poly(4,4-dimethyl-2-vinylazlactone) chains for 1 (a) and 3 min (b) and subsequently reacted with Rhodamine 6G.

irradiation time has the expected dimension of 1 mm. A desirable characteristic of the grafted features is their rather sharp boundaries perpendicular to the capillary axis.

## Conclusions

UV-initiated photografting of the pore surface of porous polymer monoliths located in capillaries is a simple and versatile approach that enables the incorporation of a broad range of surface chemistry at specific and precisely defined locations of the monolith. This straightforward in situ process is also easily adaptable to microfluidic chip technology. While this work only involved grafting using 2-acrylamido-2-methyl-1-propanesulfonic acid and 4,4-dimethyl-2-vinylazlactone, we have previously shown that the grafting ability of both of these monomers is comparable to that of a number of other monomers.<sup>22</sup> We expect that this approach will facilitate the design and preparation of numerous functional elements that can be incorporated into complex microanalytical systems as demonstrated earlier for enzymatic microreactors used for the rapid micro-scale digestion of proteins.<sup>26</sup> In contrast to the typical "homogeneous" grafting involving entire monolith, the preparation of monoliths with longitudinal gradients of surface coverage or combining different chemistries is also conceivable through the use of masks with a gradient of UV transparency. The sharp edges of the features patterned in photolithographic fashion enable the placement of different elements of a microfluidic system next to each other with no dead volume between them. Such multifunction systems involving different "photodefined" chemistries are currently under investigation. Our approach clearly opens a number of new avenues that may prove valuable in the development of low-cost functional microdevices and systems for a variety of applications.

## Experimental Section

**Materials.** 2-Acrylamido-2-methyl-1-propanesulfonic acid (99%), acetic acid (99.7%), benzamide, benzophenone (99%), 1,4-butanediol (99%), cyclohexanol (99%), 1-decanol (99%), 2,2-dimethoxy-2-phenylacetophenone (99%), phosphoric acid, Rhodamine 6G (95%), sodium carbonate, sodium sulfate, sodium tetraborate decahydrate (99.5%), and 3-(trimethoxysilyl)propyl methacrylate (98%) were purchased from Aldrich (Milwaukee, WI). Basic alumina (Brockman activity I, 60–325 mesh) was obtained from Fisher Scientific (Pittsburgh, PA). *tert*-Butyl alcohol (99.7%) was obtained from J.T. Baker (Phillipsburg, NJ), and Pluronic F-68, Gly-Tyr, Val-Tyr-Val, methionine enkephalin, and leucine enkephalin were purchased from Sigma (St. Louis, MO). 4,4-Dimethyl-2-vinylazlactone was obtained as a gift from 3M Co. (St. Paul, MN) and distilled prior use. Butyl methacrylate (99%) and ethylene dimethacrylate (98%) (both Aldrich) were purified by passing

them through a bed of basic alumina (Brockman activity I, 60–325 mesh) to remove inhibitors and distilled under reduced pressure. All other reagents were of the highest available grade and used as received.

**Light Source.** An Oriel deep UV illumination system series 8700 (Stratford, CT) fitted with a 500 W HgXe lamp was used for UV exposure. For calibration, the irradiation power was adjusted to 15.0 mW/cm<sup>2</sup>, using an OAI model 354 exposure monitor (Milpitas, CA) with a 260 nm probe head.

**Preparation of Porous Polymer Monoliths in Fused Silica Capillaries.** Fused Teflon-coated silica capillaries (50 or 100  $\mu\text{m}$  i.d., Polymicro Technologies, Phoenix, AZ) were rinsed with acetone and water using a syringe pump, activated with 0.2 mol/L sodium hydroxide for 30 min, and washed with water, then with 0.2 mol/L HCl for 30 min, then with water again, and finally with ethanol. A 20 wt % solution of 3-(trimethoxysilyl)propyl methacrylate in 95% ethanol with pH adjusted to 5 using acetic acid was pumped through the capillaries at a flow velocity of 1 mm/s for 1 h, washed with ethanol, dried in a stream of nitrogen, and left at room temperature for 24 h. The 40 cm long surface modified capillary was filled with monomer solution (Table 1) by capillary action to a length of 10.5 cm, placed under the light source, and irradiated with UV for 10 min at a distance of 30 cm. The monolith in the capillary was washed with methanol pumped through at a flow velocity of 1 mm/s for 12 h.

**Photografting of Porous Polymer Monoliths with 2-Acrylamido-2-methyl-1-propanesulfonic Acid.** A 50 or 100  $\mu\text{m}$  i.d. Teflon-coated fused silica capillary containing a porous monolith was filled with the deaerated monomer solution shown in Table 2 by pumping at a flow velocity of 1 mm/s for 30 min. Grafting was achieved by irradiation through a mask from a distance of 25 cm for a specific period of time. Alternatively, a 4 mm i.d., 6 mm o.d. quartz tube was affixed in the chuck of a mechanical stirrer and the capillary placed in this tube. These concentric tubes revolved in horizontal position at 50 rpm while irradiated. The capillary was then washed with water at a flow velocity of about 1 mm/s for 12 h and another 2 h with a 80:20 mixture of acetonitrile and 5 mmol/L phosphate buffer (pH 7).

**Photografting of Porous Polymer Monoliths with 4,4-Dimethyl-2-vinylazlactone.** The deaerated monomer solution shown in Table 2 was pumped through a 50  $\mu\text{m}$  i.d. Teflon coated fused silica capillary containing the porous monolith at a flow velocity of 1 mm/s for 30 min. The photomask was made from stripes of adhesive black tape attached to a borofloat glass wafer (100 mm  $\times$  1.1 mm, Precision Glass & Optics, Santa Ana, CA). The capillary filled with the polymerization mixture was placed under the light source, covered with the mask, and irradiated from a distance of 30 cm for a specific period of time. After the grafting was completed, the capillary was washed by acetone at a flow velocity of 1 mm/s for 12 h.

**Labeling with Rhodamine 6G.** A 0.02 mmol/L Rhodamine 6G in a standard coupling solution containing 0.5 mol/L sodium sulfate, 0.1 mol/L sodium carbonate, and 0.05 mol/L benzamide in water was prepared, filtered, and pumped through the capillaries for 4 h at 0.25  $\mu\text{L}/\text{min}$ . The capillaries were then washed with a 3:1 methanol–10 mmol/L borate buffer solution pH = 9.2 mixture for 12 h to remove the unreacted fluorescent dye.

**Electron Probe Microanalysis.** A Cameca SX-50 electron microprobe with four wavelength spectrometers operated under analytical conditions (15 keV, 20 nA) was used for detection of sulfur. The integration time was 10 s (plus 5 s for each off-peak value assuming a linear background fit) with fixed carbon and oxygen contents set at C = 70 wt % and O = 30 wt % for the matrix correction. The analyzing crystal was pentaerythritol used in a flow proportional detector, which affords a Bragg angle of  $\sin \Theta = 0.61161$ . The detection limit for sulfur in this matrix was about 150 ppm (0.004 wt %) for a single data point at a confidence of 99%.

**Porosity Measurements.** The weight of monoliths prepared in the capillaries is not sufficient for porosimetry measurement. However, we have demonstrated in our previous

work<sup>20</sup> that the porous properties of monoliths prepared in both small capillaries and bulk are very similar and therefore could mimic the conditions using polymerization in a thin mold that had a larger volume. This mold consisted of a circular Teflon plate and a quartz wafer (100  $\times$  1.6 mm, Chemglass, Vineland, NJ) separated by a 700  $\mu\text{m}$  thick polysiloxane gasket sandwiched between an aluminum base plate and a top aluminum ring held together with eight screws. The mold was filled with the polymerization mixtures (Table 1), deaerated by purging nitrogen for 10 min, and irradiated through the quartz window for 20 min. After the polymerization was completed, the mold was opened, and the solid polymer was recovered, broken into smaller pieces, extracted in a Soxhlet apparatus with methanol for 12 h, and dried in a vacuum at 60  $^{\circ}\text{C}$  for 12 h. The pore size distributions of the monolithic materials were determined using an Autopore III 9400 mercury intrusion porosimeter (Micromeritics, Norcross, GA). Scanning electron microscope (SEM) images of the morphology were obtained using an ISI high-resolution analytical scanning electron microscope DS130C (Topcon, Japan).

**Electrochromatography.** Capillary electrochromatographic experiments were carried out using an Agilent<sup>3D</sup> CE system (Agilent Technologies, Waldbronn, Germany) equipped with a diode array detector and an external pressurization system. An equal helium pressure of 0.8 MPa was applied at both ends of the capillary column. The mobile phase was prepared from phosphoric acid, which pH was adjusted to 6.0 using aqueous sodium hydroxide and then diluted to the desired concentration with a mixture of water and acetonitrile. The sample solutions (0.5 mg/mL) were injected using a pressure of 0.8 MPa for 3 s, and the separations were performed at a voltage of –15 kV while the cassette compartment temperature was adjusted to 25  $^{\circ}\text{C}$ . Acetone was used as an EOF marker.

**Acknowledgment.** This work was supported by the Office of Nonproliferation Research and Engineering of the U.S. Department of Energy under Contract DE-AC03-76SF00098 as part of a close collaboration with Sandia National Laboratory, Livermore, and by the National Institute of General Medical Sciences, National Institutes of Health (GM-48364). Support of T.R. by the Austrian Science Fund is gratefully acknowledged.

## References and Notes

- (1) Kato, K.; Uchida, E.; Kang, E. T.; Uyama, Y.; Ikada, Y. *Prog. Polym. Sci.* **2003**, *28*, 209.
- (2) Ying, L.; Wang, P.; Kang, E. T.; Neoh, K. G. *Macromolecules* **2002**, *35*, 673.
- (3) Auroux, P. A.; Iossifidis, D.; Reyes, D. R.; Manz, A. *Anal. Chem.* **2002**, *74*, 2637.
- (4) Reyes, D. R.; Iossifidis, D.; Auroux, P. A.; Manz, A. *Anal. Chem.* **2002**, *74*, 2623.
- (5) Ocvirk, G.; Verpoorte, E.; Manz, A.; Grassbauer, M.; Widmer, H. M. *Anal. Methods Instrum.* **1995**, *2*, 74.
- (6) Oleschuk, R. D.; Shultz-Lockyear, L. L.; Ning, Y. B.; Harrison, D. J. *Anal. Chem.* **2000**, *72*, 585.
- (7) Wang, C.; Oleschuk, R.; Ouchen, F.; Li, J. J.; Thibault, P.; Harrison, D. J. *Rapid Commun. Mass Spectrosc.* **2000**, *14*, 1377.
- (8) He, B.; Ji, J. Y.; Regnier, F. E. *J. Chromatogr. A* **1999**, *853*, 257.
- (9) He, B.; Tait, N.; Regnier, F. *Anal. Chem.* **1998**, *70*, 3790.
- (10) Svec, F.; Fréchet, J. M. J. *Anal. Chem.* **1992**, *54*, 820.
- (11) Svec, F.; Fréchet, J. M. J. *Science* **1996**, *273*, 205.
- (12) Svec, F.; Fréchet, J. M. J. *Ind. Eng. Chem. Res.* **1999**, *36*, 334.
- (13) Svec, F.; Fréchet, J. M. J.; Allington, R. W.; Xie, S. *Adv. Biochem. Eng. Biotechnol.* **2002**, *76*, 88.
- (14) Uyama, Y.; Kato, K.; Ikada, Y. *Adv. Polym. Sci.* **1998**, *137*, 1.
- (15) Peters, E. C.; Svec, F.; Fréchet, J. M. J.; Viklund, C.; Irgum, K. *Macromolecules* **1999**, *32*, 6377.
- (16) Viklund, C.; Ponten, E.; Glad, B.; Irgum, K.; Horsted, P.; Svec, F. *Chem. Mater.* **1997**, *9*, 463.
- (17) Lämmerhofer, M.; Peters, E. C.; Yu, C.; Svec, F.; Fréchet, J. M. J.; Lindner, W. *Anal. Chem.* **2000**, *72*, 4614.

- (18) Yu, C.; Svec, F.; Fréchet, J. M. J. *Electrophoresis* **2000**, *21*, 120.
- (19) Rohr, T.; Yu, C.; Davey, M. H.; Svec, F.; Fréchet, J. M. J. *Electrophoresis* **2001**, *22*, 3959.
- (20) Yu, C.; Xu, M.; Svec, F.; Fréchet, J. M. J. *J. Polym. Sci., Polym. Chem.* **2002**, *40*.
- (21) Rånby, B.; Yang, W. T.; Tretinnikov, O. *Nucl. Instrum. Methods Phys. Res., Sect. B* **1999**, *151*, 301.
- (22) Rohr, T.; Ogeltree, D. F.; Svec, F.; Fréchet, J. M. J. *Adv. Funct. Mater.*, in press.
- (23) Brandrup, J.; Immergut, E. H.; Grulke, E. A. In *Polymer Handbook*; Wiley: New York, 1999.
- (24) Irwan, G. S.; Kuroda, S.; Kubota, H.; Kondo, T. *J. Appl. Polym. Sci.* **2002**, *83*, 2454.
- (25) Deyl, Z.; Svec, F., Eds.; *Capillary Electrochromatography*; Elsevier: Amsterdam, 2001.
- (26) Peterson, D. S.; Rohr, T.; Svec, F.; Fréchet, J. M. J. *Anal. Chem.* **2002**, *74*, 4081.

MA021351W